Novel Route for Fabrication of ZnO nanorods-Au Nanoparticles Hybrids Directly Supported on Substrate and their Application as Gas Sensors

Gisane Gasparotto[a] , Ranilson Angelo da Silva[b], Maria Aparecida Zaghete[b], Elson Longo[b],

Leinig Antonio Perazolli[b], Talita Mazon[a]*

[a]*Centro de Tecnologia da Informação Renato Archer - CTI, Campinas, SP, Brasil*
[b]*Universidade Estadual Paulista - UNESP , Instituto de Química, Laboratório Interdisciplinar de Eletroquímica e Cerâmica - LIEC, Araraquara, SP, Brasil*

The aim of this study was to develop a novel, simple and fast route to prepare ZnO nanorods (NRs) -Au nanoparticles (NPs) hybrids directly supported on a substrate to be used in gas sensor devices. The ZnO NRs were promptly grown on interdigitated Au electrodes Al_2O_3 substrates by chemical bath deposition at a low temperature. After that, Au NPs were deposited by sputtering. Results obtained by XRD, SEM, EDX and TEM showed the perpendicularly aligned growth of the ZnO NRs with a hexagonal base on the substrate and the Au NPs homogeneously covered the ZnO NRs surface. The ZnO NRs-Au NPs hybrids-based sensor exhibited an improved sensor response for H_2 and O_2 gases compared to the ZnO NRs at 300 ºC. Due to the ability to prepare homogeneous hybrids with high surface directly supported on the substrate; the developed route might provide a convenient approach to preparing gas sensor devices.

Keywords: *ZnO, hybrids, chemical synthesis, sensor.*

1. Introduction

In the last decades, ZnO semiconductor nanostructures have drawn significant attention, mainly for their promising potential in the development of gas sensors[1-4]. The functioning of gas sensors is embedded in the changes in electrical conductivity due to adsorption / physisorption (van der Waals forces) or chemisorption (covalent bonds) processes. Electrical conductivity may also change due to reversible electrostatic attractions of reactive gases on the ZnO surface. The mechanism responsible for the semiconductors' sensitivity to gas is driven by the electrical and chemical activity of the oxygen vacancies found on the oxide surface[5].

Despite the extensive researches made about using ZnO semiconductor as gas sensors, there are still issues with long response time, slow and incomplete recovery time and low sensitivity[6]. It is well known that semiconductor oxide processing is the key to enhance gas sensor's performance. Therefore, researchers have been working in several strategies, which involve using nanostructures, doping or modifying the surface with noble metal nanoparticles aiming to get higher surface area[7-12]. For example, Au NPs have widely been used in ZnO NRs as plasma resonance to enhance the performance of ultraviolet photodetectors[3-16].

In order to ensure higher surface-to-volume ratios and one-dimensional electron mobility along growth directions and improve the sensors' characteristics, researchers have focused on making gas sensor devices from ZnO nanostructures[17-21] or ZnO nanostructures modified with Au nanoparticles (Au NPs)[8,18,22-23]. However, a number of steps are involved in preparing sensors from nanostructures or hybrids. First of all, it is necessary to synthesis of nanostructures unsupported on a substrate and posteriori deposition of Au NPs on the surface of them. After that, it occurs the preparation of a paste from nanostructures or hybrids, conformation, or deposition of it on a sensor substrate. Finally, it is necessary to realize a heat treatment to eliminate the solvent contained in it[5,7,24-29].

Because of these several steps, the preparation of homogeneous noble metal modified ZnO nanostructures with higher surface area becomes a challenge. As a consequence, the sensors show issues related to poor stability[8]. The control of the Au NPs concentration is extremely difficult by using conventional methodologies. Higher Au NPs concentrations blot out the active sites of ZnO and cause a decrease in the sensor response[22]. For that reason, the processing of nanostructured gas sensors is a challenge to be overcome aiming to reduce problems related to reproducibility and stability.

Assuming the set out above, the necessity becomes quite clear for developing a new methodology to prepare well-distributed Au nanoparticles on the surface of the ZnO nanostructures with higher surface area to improve the performance of the gas sensor based on Au NPs/ZnO hybrids[22]. Chemical bath deposition (CBD) is a simple and low-cost technique that allows synthesizing nanostructures with distinctive morphologies at low temperatures, just by changing conditions of synthesis. For this, it has been widely used to grow ZnO nanostructures on different substrates[30-31]. Chemical bath can take place in aqueous solution. The mechanism leading the formation of ZnO nanostructures

involves the crystallization, dissolution, and recrystallization phenomena[32]. On the other hand, plasma sputtering is an effective route for synthesizing Au NPs on the surface of nanostructures[6].

In this study, we report a simple and fast route, just using two steps, for producing ZnO nanorods (NRs) arrays- Au NPs hybrids directly supported on alumina substrates with interdigitated comb-like gold electrodes. Chemical bath deposition was used to grow vertically aligned ZnO nanorods supported on a substrate. Sputtering technique was used to prepare Au-NPs homogeneously distributed on the surface of the ZnO nanorods. We also investigate the enhanced resistance response of ZnO NRs-Au NPs hybrids-based sensor to H_2 and O_2 gases.

2. Experimental details

2.1 Schematic of a sensor substrate
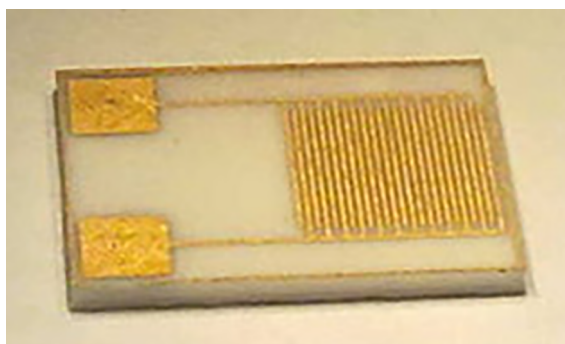
Figure 1. Schematics of a sensor substrate

Figure 1 shows a picture of the sensor substrate. It consists of interdigitated comb-like Au electrodes on the frontal side of an alumina substrate.

2.2 Synthesis of ZnO NRs-Au NPs hybrids

A solution of zinc citrate was prepared by Pechini method[33]. Zinc acetate dihydrate $((CH_3CO_2)_2Zn.2H_2O)$ was dissolved in citric acid solution and ethylene glycol in the ratio 1:4:16, respectively, with heating and stirring. The films were deposited on interdigitated Au electrodes on the alumina substrates by spin coating at 5000 rpm for 30 s. After that, the films were heat treated at 400 ºC for 3 h to be used as a seed layer.

ZnO nanorods were grown on the interdigitated Au electrodes on the alumina substrates by CBD. Potassium hydroxide solution and zinc acetate were mixed in a Teflon cup, and the sensor substrate was immersed in the solution. After, the Teflon cup was placed in a silicone bath with stirring and heating at 90 ºC for 1 hour.

Aiming to prepare ZnO NRs- Au NPs hybrids, the samples obtained by CBD were sputtered with Au for 5 seconds and heat treated at 400 ºC for 1h.

2.3 Characterization

The X-ray diffraction measurements (XRD) were taken using a diffractometer XRD Rigaku 2000 with monochromatic graphite radiation.

The microscope JEOL - JSM 7500F was used to carry out the high-resolution scanning electron microscopy and energy dispersive X-ray spectroscopy (FEG - SEM/EDX). For measurements of transmission electron microscopy (TEM) a microscope Philips CM 200 was used.

Sensing tests were performed in a test chamber. High-purity hydrogen or oxygen gas was passed through it at different flows (0.30, 0.60, 1.51, 3.06, 6.25, 16.67 cm^3/min.), controlled by a mass flow controller. Dry air (for H_2 test) or nitrogen (for O_2 test) flux of 150 cm^3/min. were used as balance gas. The sensor substrates were equilibrated in the dry air for 12 h before the beginning of gas sensor measurement to ensure a stable and reproducible baseline resistance. The electrical resistance was measured using a high-voltage source (Keithley, model 237) for all sensors. The temperature in situ was measured using a Pt/Pt-Rh (type S) thermocouples. The gas sensor measurements were performed at 200, 250 and 300 ºC for H_2 and O_2 gases. Gas sensing tests were carried out by monitoring changes of resistance during cyclic exposure to different concentrations of testing gas.

3. Results and Discussions

Figure 2 (a) shows the XRD pattern of the bare sensor substrate before the growth of the ZnO nanorods. The diffraction peaks are indexed to Ti, Au, and Al_2O_3 phases.
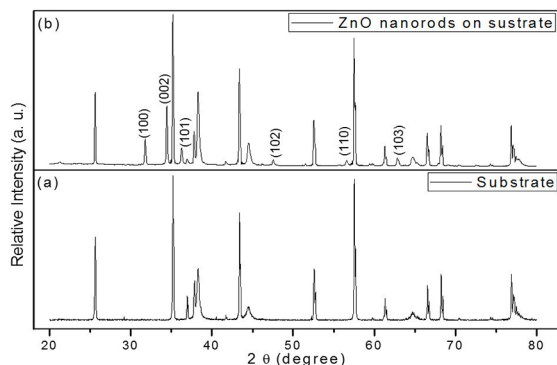
Figure 2. X-ray diffraction patterns of (a) bare sensor substrate and (b) ZnO nanorods on the substrate after chemical bath deposition

Ti and Au phases are attributed to the interdigitated gold electrode and Ti film (used to get better adhesion of the Au layer). The Al_2O_3 phase is related to the sensor substrate.

Novel ROute for Fabrication of ZnO nanorods-Au Nanoparticles Hybrids Directly Supported on Substrate and their Application as Gas Sensors

3

After ZnO nanorods growth by CBD, it is possible to identify new peaks in the XRD pattern of the sensor substrate, Figure 2 (b). The Diffraction peaks in this pattern are indexed to the hexagonal wurtzite structure ZnO, according to JCPDS 36-1451. It is possible to observe a preferential growth along the (002) plane that is characteristic of ZnO nanorods. A typical wurtzite ZnO crystal has polar faces [(002) plane] and non-polar faces [(100) and (101) planes]. The polar faces with surface dipoles are thermodynamically less stable than nonpolar faces, which tend to rearrange themselves to minimize surface energy[34]. As a result, the growth along the (002) plane shows a faster growth rate than that along other directions. This polarity causes the (002) face of the crystal to become either positively or negatively charged. In either case, the surface will attract ions O^{2-} or Zn^{2+} to it. Then, this surface covered with ions attracts other ions of opposite charges, which cover the surface, thereby resulting in the growth of the ZnO nanorods[34].

The SEM images show the morphologies of growing ZnO nanorods on Al_2O_3 substrate with interdigitated gold electrodes (Figure 3). It is possible to see that ZnO nanorods are vertically arranged, show a hexagonal shape with average diameters around 70-80 nm and length around 500 nm.

After deposition of Au film by sputtering, the samples were heated in different conditions of temperature and time. During the heated, the gold film is agglomerated to Au NPs. The distribution and size of Au nanoparticles

on the surface of ZnO nanorods may be controlled by changing the temperature of heat treatment (Figure S1). Figures 4a, 4b, 4d and 4e show the images of the ZnO NRs after Au deposition by sputtering and heated at 400 ºC. It is possible to see the presence of Au nanoparticles (black spots in TEM images) with a diameter around 5 to 10 nm on the surface of the ZnO nanorods. The Au nanoparticles homogeneously covered the ZnO nanorods surface without evidence of aggregation. The simple route developed here lead to obtain more homogenous gold particle size, and better coverage of the ZnO NRs surface compared with other methods reported throughout the literature for unsupported nanostructures[7-8,22,24-26].

EDX analysis, Figure 4.d, revealed the presence of Zn, O and Au on the sample composition. This result confirmed the presence of Au nanoparticles on the surface of the ZnO nanorods. High-resolution TEM images also confirmed these results (Figures 4.d and 4.e). The nanoparticles clearly show the crystalline structure of Au with an interplanar distance of 0.24 nm corresponding to Au (111) planes (Figure 4.d).

Response curve measurements carried out at 200 and 250 ºC showed no relevant fast response-recovery speed. So, the gas sensor measurements were performed at 300 ºC. The temporal responses of the ZnO NRs or ZnO NRs -Au NPs hybrid sensors upon exposure to different fluxes of H_2 and O_2 measured at 300 ºC are shown in Figure 5. The ZnO is a typical n-type semiconductor, and its conductivity is influenced by the surface depletion
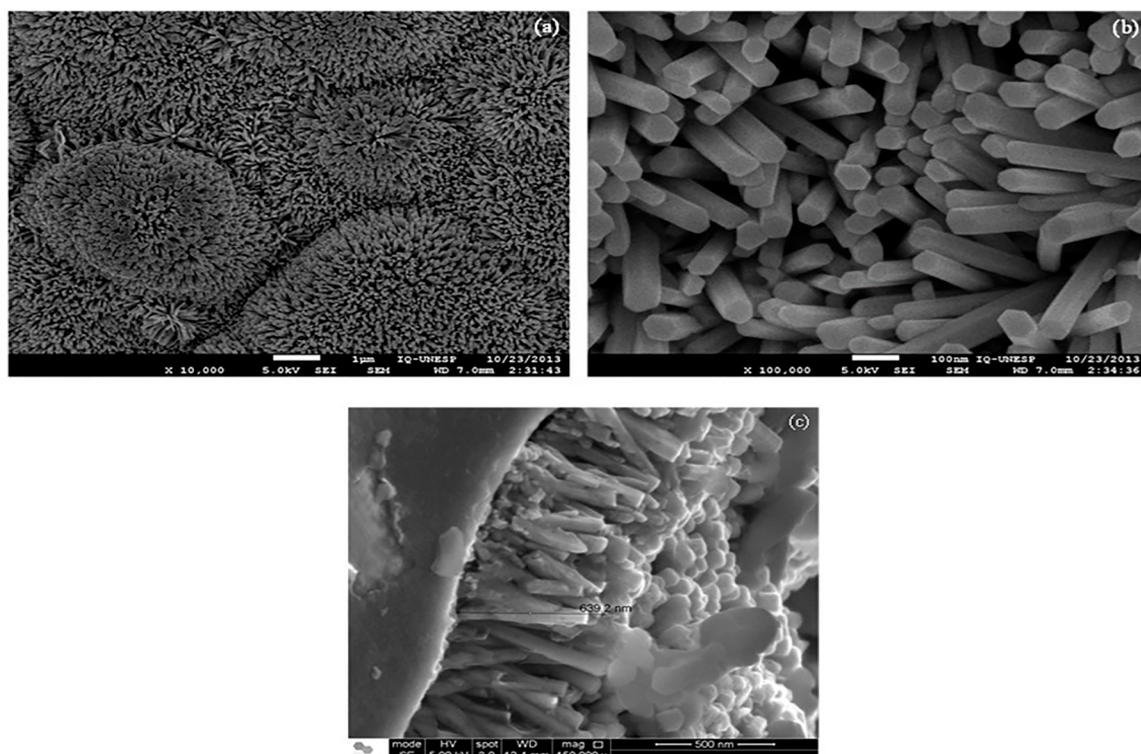
Figure 3. Scanning electron microscopy images: (a) and (b) as-prepared ZnO nanorods and (c) side view of the ZnO nanorods arrays
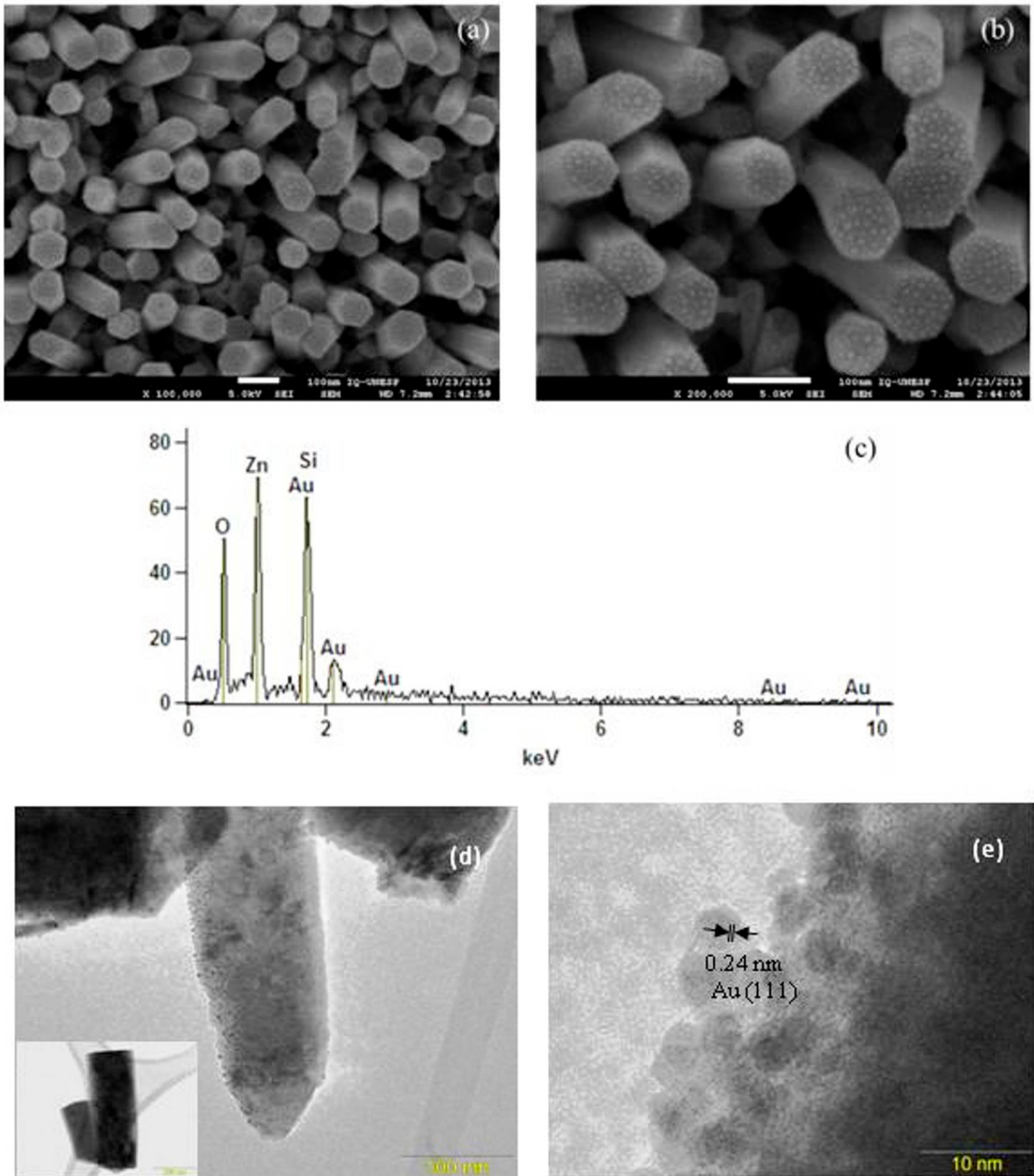
Figure 4. (a) and (b) scanning electron microscopy images of ZnO NRs- Au NPs hybrids supported on substrates, (c) energy dispersive X-ray spectroscopy spectrum of the ZnO NRs- Au NPs hybrids, (d) HRTEM image of ZnO NRs-Au NPs hybrids and (e) HRTEM Electron Diffraction of Au NPs

layer. Therefore, the mechanism of ZnO nanorods gas sensor is based upon the change of resistance. The target gas molecules adsorb onto or desorb from the working material surface (ZnO nanorods in our case), which can cause its resistivity change. Figure 5 shows the changes in resistance that are mainly induced by the adsorption and desorption of gas molecules on the surfaces of the ZnO.

In the case of exposure to H_2 reductive gas, the hydrogen molecules react with the oxygen species on

the ZnO surface. The result is a decrease in resistance (Figure 5.a). On the other hand, the oxygen molecules are adsorbed on the surfaces of ZnO to form O^-, O_2^- and O^{2-} ions by capturing electrons from the conduction band of ZnO during exposure to air. So, it is possible to observe a high-resistance state in the air[22,35]. The well-known sensing mechanism of a reduced gas is based on the interaction between adsorbed oxygen on ZnO nanorods surface and hydrogen gas. The reaction between

Novel ROute for Fabrication of ZnO nanorods-Au Nanoparticles Hybrids Directly Supported on Substrate and their Application as Gas Sensors

5
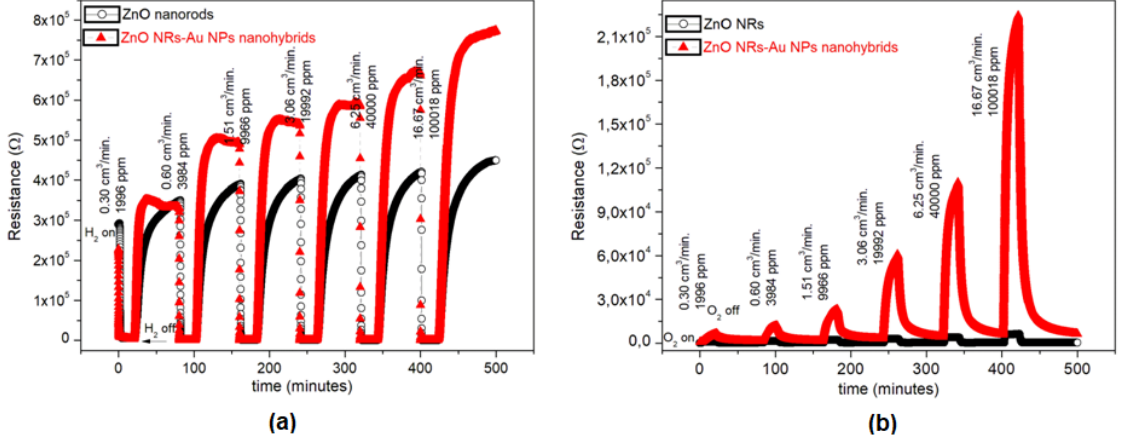
Figure 5. Resistance versus time plot for the ZnO NRs and ZnO NRs-Au NPs samples supported on Al_2O_3 in the presence of (a) H_2 and (b) O_2 at 300 °C

hydrogen and oxygen ions produces H_2O molecules and consumes adsorbed oxygen on the surface by releasing electrons (Equation 1)[6]. These electrons will return to the conduction band and cause an increase in the current of ZnO nanorods. These electrons also provide a reduction of the surface depletion region and increase the conductivity of the nanorods (Equations 2 and 3).

$$H_{2(g)} + O_o^x \leftrightarrow H_2O_{(g)} + V_o^{\cdot\cdot} \tag{1}$$

$$V_o^x \leftrightarrow V_o' + e^- \,(BC) \tag{2}$$

$$V_o' \leftrightarrow V_o'' + e^- \,(BC) \tag{3}$$
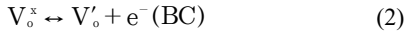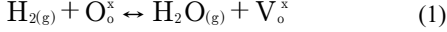
For O_2 oxidative gas, the efficiency of using ZnO NRs or ZnO NRs-Au NPs hybrids was examined by the first time in this study (Figure 5.b). Similar to the observed in the presence of hydrogen molecules, the resistance increases due to ion adsorption of oxygen species (O^-, O^{-2} and O^{2-}), the spillover effect and the influence of the Au NPs on enlarging surface space charge layer[36-38]. The interactions between adsorbed oxygen on ZnO nanorods surface and oxygen gas are the keys for the sensing mechanism of an oxidative gas (Equations 4, 5 and 6). The adsorption of O_2 molecules, which tend to trap electrons, will lead to an increase in resistance. The existence of Au makes the response amplitude changing hugely and far more evident [5].

$$O_{2(g)} \leftrightarrow O_{2(adsorbed)} \tag{4}$$

$$O_{2(adsorbed)} + e^- \leftrightarrow O_2^- \tag{5}$$

$$O_2^- + e^- \leftrightarrow 2O^- \tag{6}$$
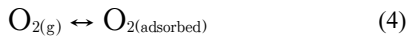
Figure 6 shows the gas sensing mechanism for the sensors considering a relative change in the depletion region of ZnO NRs and ZnO NRs- Au NPs hybrids in the presence of air, H_2 and O_2 gases.

Figure 7 shows the sensor responses as a function of H_2 and O_2 gas flow. The sensitivity or sensor response is defined as the ratio between the sensor resistance in clean air and the sensor resistance in exposed gas[39].

Compared to pure ZnO nanorods, an increase of the sensor response for the nanohybrids is observed for both gas sensors (Figure 7). This implies that ZnO NRs- Au NPs hybrid sensor is more sensitive than ZnO NRs. That's meant, ZnO NRs-Au NPs hybrid sensor has a higher degree of responsiveness to resistivity change in the presence of the gas. The improved performance of the sensor based on ZnO NRs-Au NPs hybrid is due to the highly distributed catalytic Au NPs on the ZnO nanorods. The Au NPs enhance the ionic adsorption of oxygen species (O^-, O^{-2} and O^{2-}) and the molecule-ion conversion rate[36-38]. This occurs due to the well-known spillover effect. Furthermore, the Au NPs possess a high charge storage function and act as strong acceptors of electrons[39-42]. These Au NPs's properties can induce an enlarged surface space charge layer, further resulting in the depletion of electrons near the interface.

It is possible to observe in Figure 7.a that the sensitive results obtained for the H_2 gas sensors were similar in the lowest and the highest gas flow. The difference between our results and other reported for unsupported nanostructures[22,43-44] until now, may be correlated with the thinner thickness of our device (around 800 nm) (Figure 3.c). There are, probably, enough oxygen molecules adsorbed on the surfaces of ZnO nanorods that can react with all reductive gas inside the chamber,

and it is observed no difference between the two devices at the lowest concentration. On the other hand, the Au sites become saturated quickly by the reductive gas in the highest concentration due to the thinner thickness of the device.

Although the ZnO NRs-Au NPs hybrids based-sensors show higher sensitivity to hydrogen, they also work to detect oxygen. The sensor response to O_2 gas obtained here was better than the reported throughout the literature for sensors based on Ga_2O_3 multiple nanowires[44].The higher sensitivity to oxygen is probably due to the Au NPs trap more free electrons to ZnO surface during gas-sensing measurements[36-38].

The good results obtained for sensor measurements indicate that a novel, simple and fast route developed here to prepare ZnO nanorods (NRs)-Au nanoparticles (NPs) hybrid supported on a substrate is compatible with manufacturing and process integration of gas sensor devices with excellent reproducibility, which are critical challenges in ZnO nanostructured gas sensor devices[45].

4. Conclusion

A simple, fast route was developed to prepare ZnO NRs-Au NPs hybrids supported on an alumina substrate with interdigitated comb-like Au electrodes. The Au-NPs presented diameter around 5 to 10 nm and were homogeneously distributed on the surface of the ZnO nanorods without aggregation. The prepared ZnO NRs-Au NPs hybrids -based sensor exhibited an improved sensor response for H_2 and O_2 gases compared to ZnO NRs. Due to the ability for growing high surface and homogeneous nanostructures directly on the substrate, the here developed route will provide a convenient approach to enhance the performance of the sensors.

5. Acknowledgment
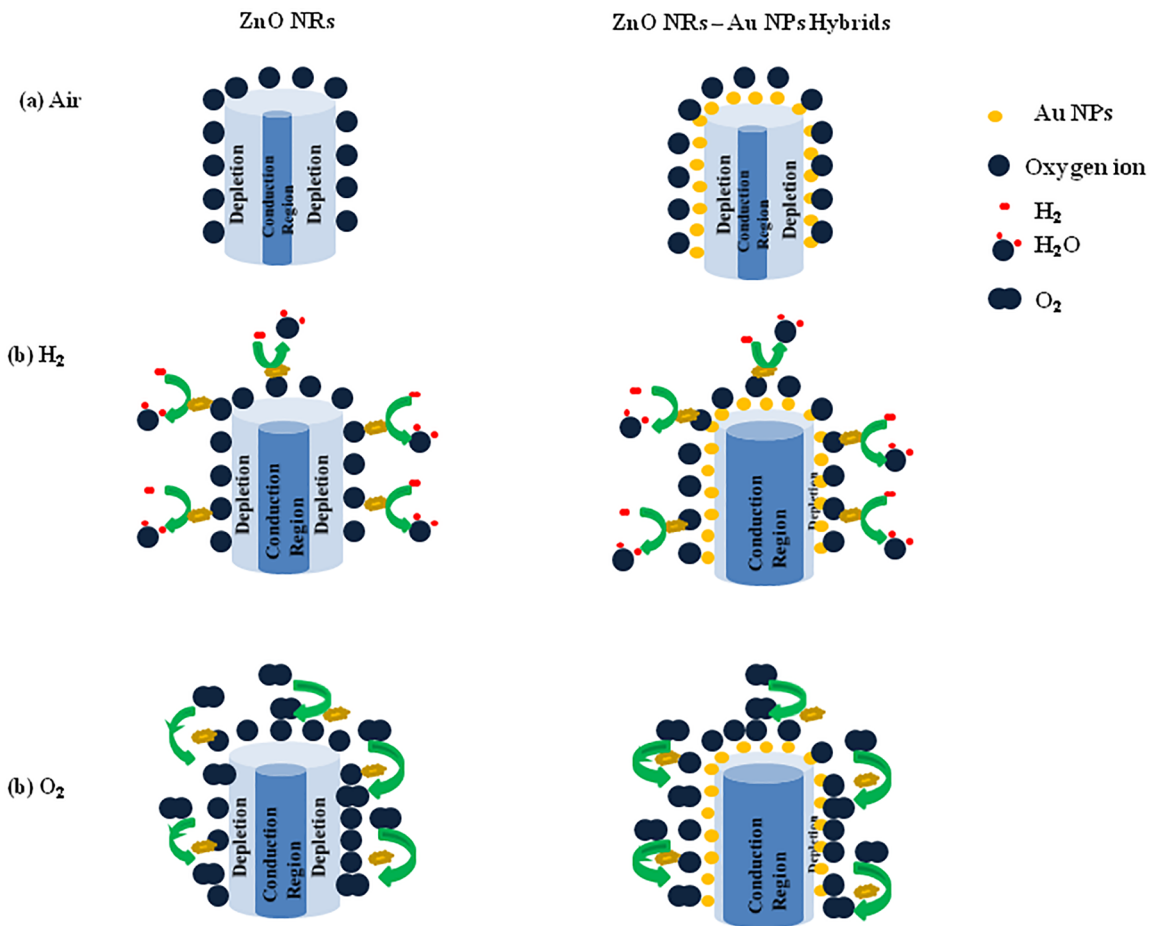
Figure 6. The gas sensing mechanism for sensor; a relative change in the depletion region of ZnO NRs and ZnO NRs- Au NPs hybrids in the presence of air, H_2 and O_2 gases
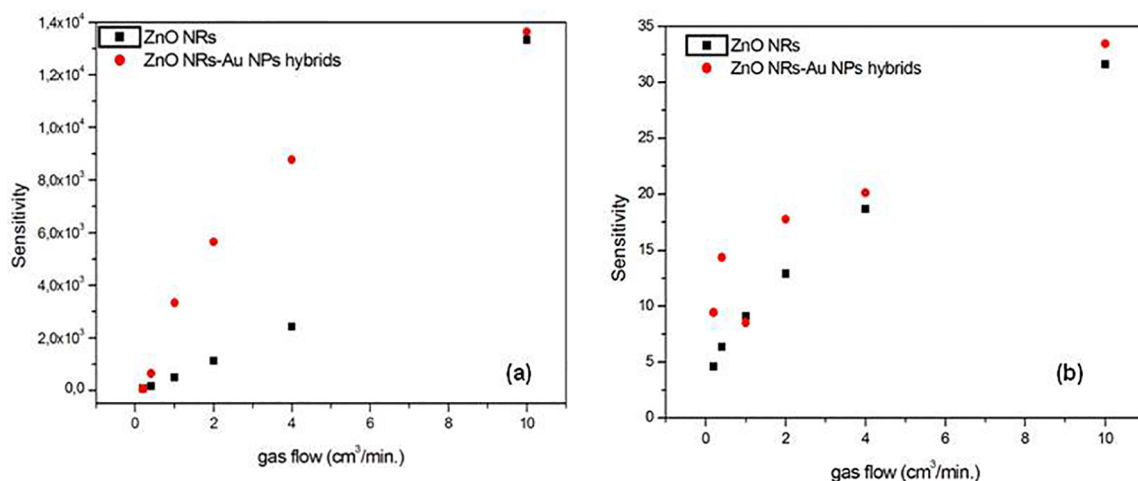
Figure 7. Relation between the sensitivity and (a) H_2 gas flow and (b) O_2 gas flow at 300 ºC

6. References

1. Ma S, Li R, Lv C, Xu W, Gou X. Facile synthesis of ZnO nanorods arrays and hierarchical nanostructures for photocatalysis and gas sensor applications. *Journal of Hazardous Materials*. 2011;192(2):730-740.

2. Cao Y, Hu X, Wang D, Sun Y, Sun P, Zheng J, et al. Flower-like hierarchical zinc oxide architecture: Synthesis and gas sensing properties. *Materials Letters*. 2012;69:45-47.

3. Rai P, Song HM, Kim YS, Song MK, Oh PR, Yoon JM, et al. Microwave assisted hydrothermal synthesis of single crystalline ZnO nanorods for gas sensor application. *Materials Letters*. 2012;68:90-93.

4. Srivastava S, Srivastava AK, Singh P, Baranwal V, Kripal R, Lee JH, et al. Synthesis of zinc oxide (ZnO) nanorods and its phenol sensing by dielectric investigation. *Journal of Alloys and Compounds*. 2015;644:597-601.

5. Wen Z, Zhu L, Zhang Z, Ye Z. Fabrication of gas sensor based on mesoporous rhombus-shaped ZnO rod arrays. *Sensors and Actuators B: Chemical*. 2015;208:112-121.

6. Drmosh QA, Yamani ZH. Synthesis, characterization, and hydrogen gas sensing properties of AuNs-catalyzed ZnO sputtered thin films. *Applied Surface Science*. 2016;375:57-64.

7. Liang YC, Liao WK, Deng XS. Synthesis and substantially enhanced gas sensing sensitivity of homogenously nanoscale Pd- an Au-particle decorated ZnO nanostructures. *Journal of Alloys and Compounds*. 2014;599:87-92.

8. Guo J, Zhang J, Zhu M, Ju D, Xu H, Cao B. High-performance gas sensor based on ZnO nanowires fuctionalized by Au nanoparticles. *Sensors and Actuators B: Chemical*. 2014;199:339-345.

9. Vijayalakshmi K, Karthick K, Gopalakrishna D. Influence of annealing on the structural, optical and photoluminescence properties of ZnO thin films for enhanced H_2 sensing application. *Ceramics International*. 2013;39(5):4749-4756.

10. Vijayalakshmi K, Renitta A. Enhanced H_2 sensing performance presented by Mg doped ZnO films fabricated with a novel ITO seed layer. *Journal of Materials Science: Materials in Electronics*. 2015;26(6):3458-3465.

11. Kashif M, Ali ME, Ali SMU, Hashim U. Sol-gel synthesis of Pd doped ZnO nanorods for room temperature hydrogen sensing applications. *Ceramics International*. 2013;39(6):6461-6466.

12. Anand K, Singh O, Singh MP, Kaur J, Singh RC. Hydrogen sensor based on graphene/ZnO nanocomposite. *Sensors and Actuators B: Chemical*. 2014;195:409-415.

13. Liu K, Sakurai M, Liao M, Aono M. Giant Improvement of the Performance of ZnO Nanowire Photodetectors by Au Nanoparticles. *Journal of Physical Chemistry C*. 2010;114(46):19835-19839.

14. Lin DD, Wu H, Zhang W, Li HP, Pan W. Enhanced UV photoresponse from heterostructured Ag-ZnO nanowires. *Applied Physics Letters*. 2009;94(17):172103.

15. Hwang JD, Wang FH, Kung CY, Chan MC. Using the Surface Plasmon Resonance of Au Nanoparticles to Enhance Ultraviolet Response of ZnO Nanorods-Based Schottky-Barrier Photodetectors. *IEEE Transactions on Nanotechnology*. 2015;14(2):318-321.

16. Hwang JD, Wang FH, Kung CY, Lai MJ, Chan MC. Annealing effects of Au nanoparticles on the surface-plasmon enhanced p-Si/n-ZnO nanorods heterojunction photodetectors. *Journal of Applied Physics*. 2014;115(17):173110.

17. Zou AL, Qiu Y, Yu JJ, Yin B, Cao GY, Zhang HQ, et al. Ethanol sensing with Au-modified ZnO microwires. *Sensors and Actuators B: Chemical*. 2016;227:65-72.

18. Ramgir NS, Sharma PK, Datta N, Kaur M, Debnath AK, Aswal DK, et al. Room temperature H_2S sensor based on Au

modified ZnO nanowires. *Sensors and Actuators B: Chemical*. 2013;186:718-726.

19. Liu XH, Zhang J, Guo XZ, Wu SH, Wang SR. Amino acid-assisted onepot assembly of Au, Pt nanoparticles onto one-dimensional ZnO microrods. *Nanoscale*. 2010;2:1178-1184.

20. Hwang IS, Kim SJ, Choi JK, Choi J, Ji H, Kim GT, et al. Synthesis and gas sensing characteristics of highly crystalline ZnO-SnO$_2$ core-shell nanowires. *Sensors and Actuators B: Chemical*. 2010;148(2):595-600.

21. Ramgir NS, Kaur M, Sharma PK, Datta N, Kailasaganapathi S, Bhattacharya S, et al. Ethanol sensing properties of pure and Au modified ZnO nanowires. *Sensors and Actuators B: Chemical*. 2013;187:313-318.

22. Tian F, Liu Y, Guo K. Au nanoparticle modified flower-like ZnO structures with their enhanced properties for gas sensing. *Materials Science in Semiconductor Processing*. 2014;21:140-145.

23. Mun Y, Park S, An S, Lee C, Kim HW. NO$_2$ gas sensing properties of Au-functionalized porous ZnO nanosheets enhanced by UV irradiation. *Ceramics International*. 2013;39(8):8615-8622.

24. Hu J, Gao F, Sang S, Li P, Deng X, Zhang W, et al. Optimization of Pd content in ZnO microstructures for high-performance gas detection. *Journal of Materials Science*. 2015;50(4):1935-1942.

25. San X, Wang G, Liang B, Song Y, Gao S, Zhang J, et al. Catalyst-free growth of one-dimensional ZnO nanostructures on SiO$_2$ substrate and in situ investigation of their H$_2$ sensing properties. *Journal of Alloys and Compounds*. 2015;622:73-78.

26. Chang CM, Hon MH, Leu IC. Influence of Size and Density of Au Nanoparticles on ZnO Nanorod Arrays for Sensing Reducing Gases. *Journal of the Electrochemical Society*. 2013;160(9):B170-B176.

27. Akermi M, Sakly N, Chaabane RB, Ouada HB. Effect of PEG-400 on the morphology and electrical properties of ZnO nanoparticles application for gas sensor. *Materials Science in Semiconductor Processing*. 2013;16(3):807-817.

28. Hussain S, Liu T, Kashif M, Lin L, Wu S, Guo W, et al. Effects of reaction time on the morphological, structural, and gas sensing properties of ZnO nanostructures. *Materials Science in Semiconductor Processing*. 2014;18:52-58.

29. Postica V, Hölken I, Schneider V, Kaidas V, Polonskyi O, Cretu V, et al. Multifunctional device based on ZnO:Fe nanostructured films with enhanced UV and ultra-fast ethanol vapour sensing. *Materials Science in Semiconductor Processing*. 2016;49:20-33.

30. Lee TH, Ryu H, Lee WJ. Fast vertical growth of ZnO nanorods using a modified chemical bath deposition. *Journal of Alloys and Compounds*. 2014;597:85-90.

31. Costa SV, Gonçalves AS, Zaghete MA, Mazon T, Nogueira AF. ZnO nanostructures directly grown on paper and bacterial cellulose substrates without any surface modification layer. *Chemical Communications*. 2013;49(73):8096-8098.

32. Issler SI, Torardi CC. Solid state chemistry and luminescence of X-ray phosphor. *Journal of Alloys and Compounds*. 1995;229(1):54-65.

33. Samanta PK, Patra SK, Chaudhuri PR. Violet emission from flower-like bundle of ZnO nanosheets. *Physica E: Low-dimensional Systems and Nanostructures*. 2009;41(4):664-667.

34. Li Q, Kumar V, Li Y, Zhang H, Marks TJ, Chang RPH. Fabrication of ZnO Nanorods and Nanotubes in Aqueus Solutions. *Chemistry of Materials*. 2005;17(5):1001-1006.

35. Zhang Y, Xu JQ, Xiang Q, Li H, Pan QY, Xu PC. Brush-Like Hierarchical ZnO Nanostructures: Synthesis, Photoluminescence and Gas Sensor Properties. *Journal of Physical Chemistry C*. 2009;113(9):3430-3435.

36. Kung MC, Davis RJ, Kung HH. Understanding Au-catalyzed low-temperature CO oxidation. *Journal of Physical Chemistry C*. 2007;111(32):11767-11775.

37. Joshi RK, Hu Q, Alvi F, Joshi N, Kumar A. Au Decorated Zinc Oxide Nanowires for CO Sensing. *Journal of Physical Chemistry C*. 2009;113(36):16199-16202.

38. Im J, Singh J, Soares JW, Steeves DM, Whitten JE. Synthesis and Optical Properties of Dithiol-Linked ZnO/Gold Nanoparticle Composites. *Journal of Physical Chemistry C*. 2011;115(21):10518-10523.

39. Li CC, Yin XM, Li QH, Wang TH. Enhanced gas sensing properties of ZnO/SnO2 hierarchical architectures by glucose-induced attachment. *CrystEngComm*. 2011;13(5):1557-1563.

40. Subramanian V, Wolf EE, Kamat PV. Green Emission to Probe Photoinduced Charging Events in ZnO-Au Nanoparticles: Charge Distribution and Fermi-Level Equilibration. *Journal of Physical Chemistry B*. 2003;107(30):7479-7485.

41. Yang TT, Chen WT, Hsu YJ, Wei KH, Lin TY, Lin TW. Interfacial Charge Carrier Dynamics in Core-Shell Au-CdS Nanocrystals. *Journal of Physical Chemistry C*. 2010;114(26):11414-11420.

42. Wang C, Wei YJ, Jiang HY, Sun SH. Tug-of-War in Nanoparticles: Competitive Growth of Au on Au-Fe$_3$O$_4$ Nanoparticles. *NanoLetters*. 2009;9(12):4544-4547.

43. Li X, Zhou X, Guo H, Wang C, Liu J, Sun P, et al. Design of Au@ZnO Yolk-Shell Nanospheres with Enhanced Gas Sensing Properties. *Applied Materials and Interfaces*. 2014;6(21):18661-18667.

44. Liu Z, Yamazaki T, Shen Y, Kikuta T, Nakatani N, Li Y. O$_2$ and CO sensing of Ga$_2$O$_3$ multiple nanowire gas sensors. *Sensors and Actuators B: Chemical*. 2008;129(2):666-670.

45. Tiwale N. Zinc oxide nanowire gas sensors: fabrication, functionalisation and devices. *Materials Science and Technology*. 2015;31(14):1681-1697.Supplementary Material

Supplementary Material

The following online material is available for this article:

Figure S1 - SEM images of the ZnO NRs- Au NPs hybrids supported on substrates heat treated at different temperatures (a) 350 ºC, (b) 450 ºC, and (c) 550 ºC